Scientia Pharmaceutica

ÖSTERREICHISCHE PHARMAZEUTISCHE GESELLSCHAFT

MDPI

Article

Synthesis and Biological Activity Evaluation of Novel 5-Methyl-7-Phenyl-3*H*-Thiazolo[4,5-*b*]Pyridin-2-Ones

Andrii Lozynskyi [1], Yulian Konechnyi [2], Julia Senkiv [3], Ihor Yushyn [1], Dmytro Khyluk [4], Olexandr Karpenko [5], Yulia Shepeta [6] and Roman Lesyk [1,7,*]

1 Department of Pharmaceutical, Organic and Bioorganic Chemistry, Danylo Halytsky Lviv National Medical University, 69 Pekarska, 79010 Lviv, Ukraine; lozynskyiandrii@gmail.com (A.L.); ihor.yushyn@gmail.com (I.Y.)
2 Department of Microbiology, Danylo Halytsky Lviv National Medical University, 69 Pekarska, 79010 Lviv, Ukraine; yuliankonechnyi@gmail.com
3 Institute of Cell Biology, NAS of Ukraine, 14/16 Drahomanova, 79005 Lviv, Ukraine; yu.senkiv@gmail.com
4 Department of Organic Chemistry, Medical University of Lublin, Aleje Racławickie 1, 20-059 Lublin, Poland; dmytrokhylyuk@gmail.com
5 Enamine Ltd., 23 Alexandra Matrosova, 01103 Kyiv, Ukraine; karalexander@gmail.com
6 Department of Pharmaceutical Chemistry, National Pirogov Memorial Medical University, 56 Pirogov, 21018 Vinnytsya, Ukraine; shepeta.yulia@gmail.com
7 Department of Biotechnology and Cell Biology, Medical College, University of Information Technology and Management in Rzeszow, Sucharskiego 2, 35-225 Rzeszow, Poland
* Correspondence: dr_r_lesyk@org.lviv.net; Tel.: +38-032-275-5966

Abstract: A series of 5-methyl-7-phenyl-3*H*-thiazolo[4,5-*b*]pyridin-2-ones has been designed, synthesized, and characterized by spectral data. Target compounds were screened for their antimicrobial activity against some pathogenic bacteria and fungi, and most of them showed moderate activity, especially compound **3g**, which displayed the potent inhibitory effect against *Pseudomonas aeruginosa* and *Escherichia coli* with MIC value of 0.21 μM. The active thiazolopyridine derivatives **3c**, **3f**, and **3g** were screened for their cytotoxicity effects on HaCat, Balb/c 3T3 cells using MTT assay, which revealed promising results. In silico assessment for compounds **3c**, **3f**, and **3g** also revealed suitable drug-like parameters and ADME properties. The binding interactions of the most active compound **3g** were performed through molecular docking against MurD and DNA gyrase, with binding energies and an inhibitory constant compared to the reference drug ciprofloxacin. The tested thiazolo[4,5-*b*]pyridines constitute an exciting background for the further development of new synthetic antimicrobial agents.

Keywords: thiazolo[4,5-*b*]pyridines; antimicrobial activity; pharmacokinetics prediction; molecular docking

Citation: Lozynskyi, A.; Konechnyi, Y.; Senkiv, J.; Yushyn, I.; Khyluk, D.; Karpenko, O.; Shepeta, Y.; Lesyk, R. Synthesis and Biological Activity Evaluation of Novel 5-Methyl-7-Phenyl-3*H*-Thiazolo[4,5-*b*]Pyridin-2-Ones. *Sci. Pharm.* **2021**, *89*, 52. https://doi.org/10.3390/scipharm89040052

Academic Editor: Thierry Besson

Received: 26 October 2021
Accepted: 23 November 2021
Published: 25 November 2021

1. Introduction

Pyridine-based derivatives are a known class of heterocyclic compounds that underly the structure of many vitamins, alkaloids, disinfectants, herbicides, and medicines [1,2]. The pharmacological significance of these compounds is related to easy metabolism in the human body by N-methylation and N- and C-oxidation pathways [3]. On the other hand, the toxic effect of these compounds is also well established [4,5]. It is worth mentioning that the main interest in searching for pharmacologically attractive pyridines is devoted to their condensed analogs due to their diverse biological activity and clinical applications. Thus, condensed heterocyclic systems with a pyridine moiety in the structure occur in many commercially available drugs with different mechanisms of biological activity (Figure 1). In addition, fused pyridine-based heterocycles have been identified as potent antimicrobial [6,7], anticancer [8,9], antichagasic [10], antioxidant [11,12], and anti-inflammatory agents [13,14]. Furthermore, some fused pyridine derivatives were found to be inhibitors of glycogen synthase kinase-3 (GSK-3) [15], CDK5 protein kinase [16],

tyrosyl-tRNA synthetase [17], cdc2-like kinase 1 (CLK1) [18], and tumor necrosis factor-α (TNF-α) [19].

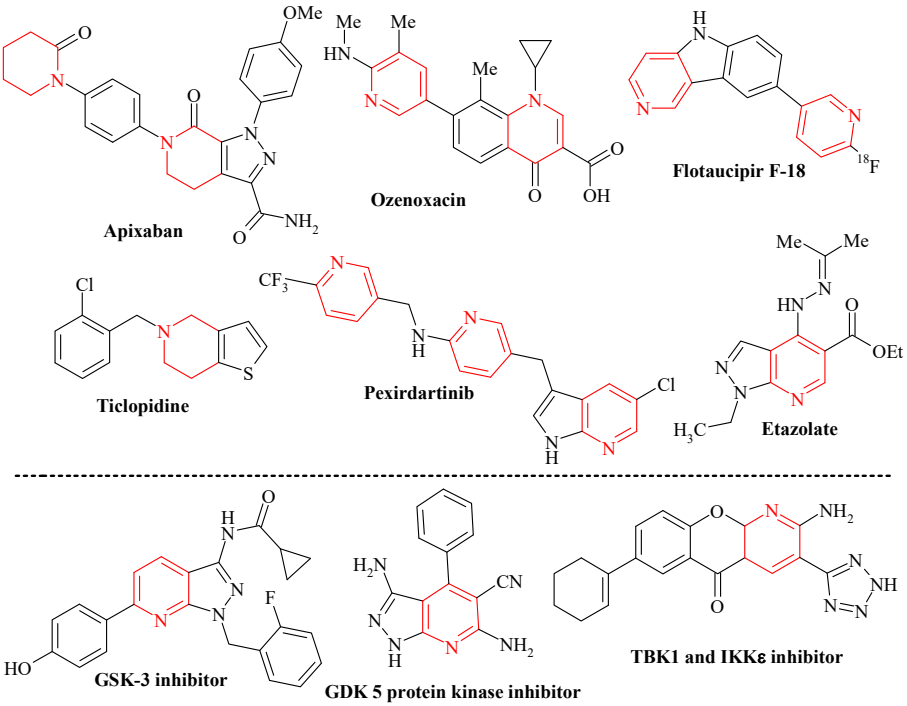

Figure 1. Structures of biologically active fused pyridine derivatives.

The effective way to obtain potential drug-like molecules, including fused pyridine derivatives, is through the reactions of aminoazoles as binucleophiles with various electrophiles [20–22]. The reactions of aminoazoles with α,β-unsaturated aldehydes and ketones, α-ketoacids, ketoesters, β-dicarbonyls yielding fused pyridine derivatives have been reported previously [23–25] (Figure 2). The mentioned carbonyl compounds with an unsaturated chain are also effective reagents in other pericyclic reactions, especially the Diels–Alder reaction with dienophiles in constructing different polycyclic systems [26–28].

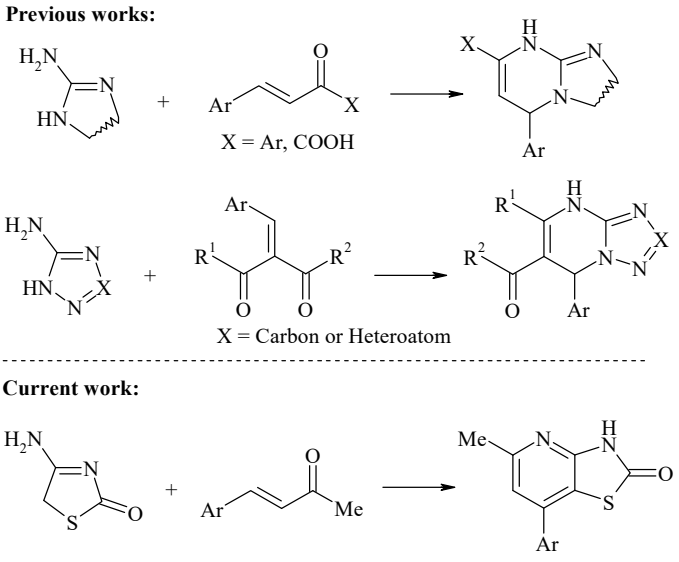

Figure 2. Background for target compounds synthesis.

The current work is devoted to the synthesis and study of the biological activity of condensed pyridine derivatives, namely thiazolopyridines. Thus, a combination of

thiazole ring with biologically relevant pyridine fragment is a practical direction in creating potential biologically active compounds within a hybrid-pharmacophore approach. This approach allows for the obtaining of new classes of organic compounds with enhanced activity and reduced toxicity [29]. Some thiazolopyridines have been studied successfully as antioxidant [30], anti-inflammatory [31], antifungal [32], and herbicidal agents [33]. In addition, in our previous studies, we reported the synthesis of thiazolo[4,5-*b*]pyridines via the [3 + 3]-cyclization of 4-amino-5*H*-thiazol-2-one and chalcones and arylidene pyruvic acids (APAs), which demonstrated anticancer [25,34] and antimicrobial activities [35].

Given our interest in searching and studying new low molecular weight compounds among fused pyridines, herein, we report the synthesis, structure elucidation, and in vitro antimicrobial, cytotoxic activity evaluation and docking studies of some novel 5-methyl-7-phenyl-3*H*-thiazolo[4,5-*b*]pyridin-2-ones. This manuscript is intended to draw attention to the chemistry and pharmacology of the thiazolopyridines and its further examination as potent drug candidates.

2. Materials and Methods

2.1. General Information

All materials were purchased from commercial sources and used without purification. Melting points were measured in open capillary tubes and were uncorrected. The elemental analyses were performed using the Thermo Scientific FlashSmart Elemental Analyzer. The ^{1}H and ^{13}C NMR spectra were recorded on Varian Gemini (^{1}H at 400 and ^{13}C at 100 MHz) instrument in DMSO-d_6. Chemical shifts (δ) are given in ppm units relative to tetramethylsilane as reference (0.00). LC-MS was performed using a system with an Agilent 1100 Series HPLC equipped with diode-array detector and Agilent LC\MSD SL mass-selective detector using chemical ionization at atmospheric pressure (APCI). The reaction mixture was monitored by thin-layer chromatography (TLC) using Silufol-254 plates. Starting 4-amino-5*H*-thiazol-2-one and benzylideneacetones were prepared according to reported methods [36,37].

2.2. Synthesis and Characterization of Compounds

General Procedure for the Synthesis of
5-Methyl-7-Phenyl-3*H*-Thiazolo[4,5-*b*]Pyridin-2-Ones **3a**–**g**

A mixture of benzylideneacetone (1.0 mmol) and 4-amino-5*H*-thiazol-2-one (1.0 mmol) was refluxed for 3 h in glacial acetic acid (10 mL) (monitored by TLC). After completion, the reaction mixture was cooled and left overnight at room temperature. The solid precipitates were filtered off, washed with methanol (5–10 mL), and recrystallized from a mixture of DMF: acetic acid (1:2) or glacial acetic acid. The resulting powders were filtered and washed with acetic acid, water, methanol, and diethyl ether, successively. The final products were dried at room temperature until constant weight.

7-(4-Methoxyphenyl)-5-methyl-3*H*-thiazolo[4,5-*b*]pyridin-2-one (**3a**). Yield 71%, mp > 240 °C (AcOH). ^{1}H NMR (400 MHz, DMSO-d_6): δ 2.47 (s, 3H, CH_3), 3.82 (s, 3H, OCH_3), 7.10 (d, 2H, *J* = 8.6 Hz, arom.), 7.15 (s, 1H, CH), 7.59 (d, 2H, *J* = 8.6 Hz, arom.), 12.55 (s, 1H, NH). ^{13}C NMR (100 MHz, DMSO-d_6): δ 23.8, 55.8, 113.4, 115.1, 117.1, 129.2, 131.8, 138.6, 143.2, 150.4, 153.4, 160.6. ESI-MS m/z 273 $(M + H)^+$. Anal. Calcd for $C_{14}H_{12}N_2O_2S$: C, 61.75; H, 4.44; N, 10.29. Found: C, 61.62; H, 4.34; N, 10.38.

7-(4-Dimethylaminophenyl)-5-methyl-3*H*-thiazolo[4,5-*b*]pyridin-2-one (**3b**). Yield 74%, mp > 240 °C (DMF:EtOH). ^{1}H NMR (400 MHz, DMSO-d_6): δ 2.45 (s, 3H, CH_3), 2.97 (s, 6H, $N(CH_3)_2$), 6.83 (d, 2H, *J* = 8.8 Hz, arom.), 7.12 (s, 1H, CH), 7.50 (d, 2H, *J* = 8.8 Hz, arom.), 12.48 (s, 1H, NH). ^{13}C NMR (100 MHz, DMSO-d_6): δ 23.7, 37.4, 112.6, 116.2, 123.5, 128.6, 136.6, 143.6, 146.0, 151.4, 156.8, 162.0. ESI-MS m/z 286 $(M + H)^+$. Anal. Calcd for $C_{15}H_{15}N_3OS$: C, 63.13; H, 5.30; N, 14.72. Found: C, 63.22; H, 5.40; N, 14.68.

7-(4-Fluorophenyl)-5-methyl-3*H*-thiazolo[4,5-*b*]pyridin-2-one (**3c**). Yield 67%, mp 220–222 °C (AcOH). ^{1}H NMR (400 MHz, DMSO-d_6): δ 2.48 (s, 3H, CH_3), 7.18 (s, 1H, CH), 7.38 (t, 2H, *J* = 8.8 Hz, arom.), 7.68 (dd, 2H, *J* = 5.3, 8.8 Hz, arom.), 12.55 (s, 1H, NH). ^{13}C

NMR (100 MHz, DMSO-d_6): δ 20.0, 110.7, 116.8, 124.3, 130.2, 142.4 (d, J = 6.0 Hz, C–F), 144.8, 157.5 (d, J = 30.0 Hz, C–F), 162.9, 165.2, 166.5 (d, J = 220.0 Hz, C–F), 169.1. ESI-MS m/z 261 $(M + H)^+$. Anal. Calcd for $C_{13}H_9FN_2OS$: C, 59.99; H, 3.49; N, 10.76. Found: C, 60.09; H, 3.32; N, 10.68.

7-(3-Hydroxy-4-methoxyphenyl)-5-methyl-3*H*-thiazolo[4,5-*b*]pyridin-2-one (**3d**). Yield 65%, mp > 240 °C (AcOH). ^{1}H NMR (400 MHz, DMSO-d_6): δ 2.38 (s, 3H, CH_3), 3.81 (s, 3H, OCH_3), 7.03–7.05 (m, 3H, arom.), 7.09 (s, 1H, CH), 9.36 (s, 1H, OH), 12.49 (s, 1H, NH). ^{13}C NMR (100 MHz, DMSO-d_6): δ 21.1, 56.1, 113.0, 119.0, 122.5, 129.5, 130.8, 138.4, 143.4, 147.4, 149.2, 153.6, 165.6, 169.3. ESI-MS m/z 289 $(M + H)^+$. Anal. Calcd for $C_{14}H_{12}N_2O_3S$: C, 58.32; H, 4.20; N, 9.72. Found: C, 58.45; H, 4.32; N, 9.61.

7-(4-Chlorophenyl)-5-methyl-3*H*-thiazolo[4,5-*b*]pyridin-2-one (**3e**). Yield 73%, mp > 240 °C (DMF:EtOH). ^{1}H NMR (400 MHz, DMSO-d_6): δ 2.49 (s, 3H, CH_3), 7.20 (s, 1H, CH), 7.61–7.68 (m, 4H, arom.), 12.64 (s, 1H, NH). ^{13}C NMR (100 MHz, DMSO-d_6): δ 23.8, 117.4, 120.1, 129.6, 129.7, 134.7, 135.8, 142.1, 156.6, 160.1, 163.4. ESI-MS m/z 277/279 $(M + H)^+$. Anal. Calcd for $C_{13}H_9ClN_2OS$: C, 56.42; H, 3.28; N, 10.12. Found: C, 56.30; H, 3.34; N, 10.19.

7-(4-Bromophenyl)-5-methyl-3*H*-thiazolo[4,5-*b*]pyridin-2-one (**3f**). Yield 74%, mp > 240 °C (DMF:EtOH). ^{1}H NMR (400 MHz, DMSO-d_6): δ 2.49 (s, 3H, CH_3), 7.21 (s, 1H, CH), 7.59 (d, 2H, J = 8.4 Hz, arom.), 7.76 (d, 2H, J = 8.4 Hz, arom.), 12.64 (s, 1H, NH). ^{13}C NMR (100 MHz, DMSO-d_6): δ 23.8, 115.4, 117.3, 123.4, 129.9, 132.7, 136.2, 142.2, 150.9, 165.2, 169.0. ESI-MS m/z 321/323 $(M + H)^+$. Anal. Calcd for $C_{13}H_9BrN_2OS$: C, 48.61; H, 2.82; N, 8.72. Found: C, 48.52; H, 2.91; N, 8.59.

7-(3,4-Dimethoxyphenyl)-5-methyl-3*H*-thiazolo[4,5-*b*]pyridin-2-one (**3g**). Yield 68%, mp 236–238 °C (AcOH). ^{1}H NMR (400 MHz, DMSO-d_6): δ 2.40 (s, 3H, CH_3), 3.82 (s, 3H, OCH_3), 3.83 (s, 3H, OCH_3), 7.13 (s, 1H, CH), 7.19–7.21 (m, 3H, arom.), 12.54 (s, 1H, NH). ^{13}C NMR (100 MHz, DMSO-d_6): δ 27.6, 54.5, 56.0, 110.8, 112.0, 123.4, 125.6, 127.5, 143.9, 149.4, 151.4, 155.0, 158.6, 162.7, 164.9. ESI-MS m/z 303 $(M + H)^+$. Anal. Calcd for $C_{15}H_{14}N_2O_3S$: C, 55.59; H, 4.67; N, 9.27. Found: C, 55.40; H, 4.54; N, 9.19.

2.3. Antimicrobial Activity

The synthesized compounds were tested in vitro for their antibacterial and antifungal activities using the agar diffusion and serial dilutions resazurin-based microdilution assays (RBMA) [38,39]. For this purpose, 100 μL (1 mg/mL) of the tested compound was placed in an agar well with a diameter of 5.5 mm. The diameter of the growth retardation was measured using a micrometer with an error of 0.1 mm. Dimethyl sulfoxide (DMSO), vancomycin (discs), ciprofloxacin (discs), and clotrimazole (discs) were used as a control. Pure DMSO was used as a solvent due to the poor solubility of the test compounds in dilute DMSO. In addition, Mueller–Hinton agar and Saburo agar (for fungi) were used, and Petri dishes were incubated at 37 °C for 24 h for bacteria and at 25 °C for 24–48 h for fungi. The RBMA method involved the introduction of a 96-well plate 50 μL of nutrient medium (Mueller–Hinton broth or glucose broth), 50 mL of a suspension of the microorganism (McFarland 2.0), and 100 μL of tested compounds, with the addition of 15 μL of 0.02% resazurin in each well. Sixteen reference and clinical microbial and fungal strains were used (Table 1), previously identified by the MALDI TOF system (Bruker, Bremen, Germany), and 16S rRNA gene sequences. All clinical strains were multidrug-resistant or extensively drug-resistant with different antibiotic resistance patterns. Clinical strains were isolated from a patient with healthcare-associated infections from regional hospitals. All testing was repeated in triplicate.

Table 1. In vitro antimicrobial activity of synthesized compounds (zone of growth inhibition at conc. 1 mg/mL after 24–48 h).

	Type of Species		Species of Bacteria and Fungi	Zone of Growth Inhibition (mm ± SE)										
				3a	3b	3c	3d	3e	3f	3g	DMSO	Vancomycin	Ciprofloxacin	Clotrimazole
1	Gram-negative bacteria	Reference strains	*Pseudomonas aeruginosa* (ATCC 27853 (F-51))	00	00	00	00	00	7.0 ± 0.3 **	9.0 ± 0.4 **	00	-	35.0 ± 0.3	-
2			*Escherichia coli* (ATCC 25922)	7.0 ± 0.25 **	00	7.0 ± 0.3 **	00	7.0 ± 0.2 **	00	00	00	-	42.0 ± 0.5	-
3			*Raoultella terrigena* (ATCC 33257)	11.0 ± 0.4 **	00	11.6 ± 0.3 **	00	00	11.2 ± 0.4 **	00	00	-	30.0 ± 0.5	-
4		Clinical strains	*Pseudomonas aeruginosa* N 7	9.2 ± 0.2	9.2 ± 0.2	9.2 ± 0.3 **	9.2 ± 0.2	9.2 ± 0.2	9.5 ± 0.3	10.5 ± 0.4 *	9.2 ± 0.2	-	20.0 ± 0.2	-
5			*Escherichia coli* N 37	11.6 ± 0.25 **	00	9.2 ± 0.2 **	00	00	00	9.9 ± 0.2 **	00	-	14.0 ± 0.4	-
6			*Raoultella terrigena* N1	12.0 ± 0.5 **	00	00	00	00	12.0 ± 0.3**	00	00	-	12.0 ± 0.3	-
7			*Achromobacter xylosoxidans* N 147	10.0 ± 0.4 **	8.0 ± 0.3	12.8 ± 0.3 **	10.0 ± 0.4 **	8.0 ± 0.3	8.0 ± 0.3	11.0 ± 0.2 **	8.0 ± 0.2	-	15.0 ± 0.5	-
8			*Citrobacter freundii* N 2	7.7 ± 0.2	7.7 ± 0.2	9.0 ± 0.5 *	10.8 ± 0.4 **	7.7 ± 0.2	11.8 ± 0.4**	11.8 ± 0.5 **	7.7 ± 0.2	-	16.0 ± 0.3	-
9	Gram-positive bacteria	Reference strain	*Staphylococcus aureus* (ATCC 25923 (F-49))	00	00	11.2 ± 0.5	12.0 ± 0.3	00	11.2 ± 0.3	00	11.2 ± 0.4	32 ± 0.5	35.0 ± 0.5	-
10		Clinical strains	*Staphylococcus aureus* N 23	00	00	12.0 ± 0.3	12.2 ± 0.4	00	11.4 ± 0.3	00	11.6 ± 0.2	11.4 ± 0.3	9.0 ± 0.2	-
11			*Kocuria marina* N 133	00	00	12.2 ± 0.4 **	00	00	00	00	00	25.1 ± 0.4	8.0 ± 0.2	-
12			*Micrococcus luteus* N 136	00	00	00	00	00	00	10.2 ± 0.4 **	7.0 ± 0.3	12.0 ± 0.2	10.0 ± 0.2	-
13	Fungi	Reference strain	*Candida. albicans* (ATCC 885-653)	14.4 ± 0.4 **	14.5 ± 0.5 **	00	9.6 ± 0.3	12.7 ± 0.4 **	9.7 ± 0.3	12.2 ± 0.2	9.7 ± 0.2 **	-	-	18.0 ± 0.5
14		Clinical strains	*Candida albicans* N 60	00	00	9.7 ± 0.3	9.2 ± 0.4 **	00	11.2 ± 0.5 **	9.0 ± 0.3 **	00	-	-	11.0 ± 0.3
15			*Candida kefyr* N 68	13.8 ± 0.1 **	12.3 ± 0.4	9.8 ± 0.4 **	14.5 ± 0.4 **	14.9 ± 0.3 **	14.6 ± 0.2 **	14.7 ± 0.2 **	12.5 ± 0.2	-	-	6.0 ± 0.2
16			*Saccharomyces cerevisiae* N 62	00	00	12.5 ± 0.4 **	8,0 ± 0.2 **	00	8,0 ± 0.2 **	00	00	-	-	8.0 ± 0.2

Vancomycin 30 µg (inhibition zone 17–21 mm for *S. aureus*); Ciprofloxacin 5 µg (inhibition zone 25–33 mm for *P. aeruginosa*, 22–30 mm for *S. aureus*, 30–40 mm for *E.coli*); Clotrimazole 10 µg (inhibition zone 12–17 mm for *Candida* spp; * $p < 0.05$; ** $p < 0.001$, compare to DMSO; diameter of well 5.5 mm.

2.4. MTT Assay

The cytotoxic effect of new thiazolopyridine derivatives on pseudonormal cell lines was evaluated using MTT assay. The 4×10^4 cells/mL human epidermal keratinocytes (HaCat cell line) or normal murine fibroblasts (BALB/c 3T3 cell line) were seeded in 96-well plates in 100 µL DMEM medium, supplemented with 10% FBS and incubated for 24 h to attach at 37C in CO_2 incubator. The HaCaT human skin keratinocyte cell line and normal murine fibroblasts (BALB/c 3T3) were kindly gifted by the R.E. Kavetsky Institute of experimental pathology, oncology and radiobiology NAS of Ukraine (Kyiv, Ukraine). The next day, they were treated with studied compounds at concentrations 10, 25, 50, 150, and 250 µM. After 72 h compound exposure, 20 µL MTT reagent was added, incubated for 4 h, and measured according to the manufacturer's recommendations (Merck KGaA, Burlington, MA, USA).

2.5. Molecular Docking

Molecular docking is the most widespread method for the calculation and prediction of protein–ligand interactions. Before docking procedures, we analyzed available literature data for choosing the most logical and appropriate biological targets. There are literally reported 4-thiazolidinones derivatives, which demonstrate antibacterial activities through MurD ligase inhibition [40]. Moreover, the well-known DNA gyrase inhibitors fluoroquinolones are based on the core, which are quite similar to 3*H*-thiazolo[4,5-*b*]pyridin-2-one. Additionally, structurally related 4,5,6,7-tetrahydrobenzo[1,2-*d*]thiazole-based derivatives were identified as DNA gyrase inhibitors [41]. That is why MurD ligase (PBD code 2Y67) [42] and DNA gyrase (PBD code 2XCT) [43] were chosen for docking in silico simulations with the aim of receiving the necessary data for a suggestion about the possible mechanism of antibacterial activity for our lead compound **3g**.

The X-ray crystal structures of target proteins were downloaded from the Protein Data Bank (RCSB PDB: Homepage. Available online: https://www.rcsb.org/ (accessed on 20 August 2021)). The AutoDock Tools were used for preparing the enzymes for docking, which includes removing all bound ligands and water molecules, adding polar hydrogen atoms, and defining all rotatable bonds [44]. Moreover, Kollman charges were computed and spread over all atoms in residues. The chemical structure of **3g** was made using Biovia Draw and energy minimization was carried out by Hyperchem 7.5 using an AM1 quantum technique until the RMS gradient was less than 0.01 kcal /(mol Å). The three-dimensional grid boxes were created with the size $50 \times 50 \times 50$ xyz points, the spacing between grid points was 0.375 Å, and the grid maps representing the intact ligand in the actual docking target site were made by Auto Grid Tool. For more accurate results, we changed Lamarckian Genetic Algorithm (LGA) parameters from the default setting to enhanced, including 100 runs, 300 populations, and 2,50,0000 energy evaluations, a mutation rate of 0.02, and a crossover rate of 0.80 [45]. The interactions were estimated in terms of binding energy (kcal/mol) and inhibition constant (µM) along with the number of hydrogen bonds formed with the surrounding amino acid residues. The validations of selected docking parameters were performed by redocking of the initial ligands from the used enzyme structures. The accuracies of the redocking experiments were assessed by calculating the root-mean-square deviations (RMSD) and cutting off the results with RMSD > 2. Visualization and interpretation of obtained data were performed by Discovery Studio Visualizer of Dassault Systemes Biovia ® (Vélizy-Villacoublay, Yvelines, France).

3. Results and Discussion

3.1. Synthesis

In this article, we performed the condensation reaction of 4-amino-5*H*-thiazol-2-one with benzylideneacetone, leading to 5-methyl-7-phenyl-3*H*-thiazolo[4,5-*b*]pyridin-2-ones using conventional thermal heating conditions (Scheme 1). The starting benzylideneacetones **2a**–**g** were synthesized according to the known literature procedures by reaction of aromatic aldehydes and acetone in an aqueous solution of potassium hydroxide and

were subsequently used directly without additional purification. Analytical and spectral data (^{1}H and ^{13}C NMR) confirmed the structure of the synthesized compounds (copies of the corresponding spectra are presented in the Supplementary Material). The ^{1}H NMR spectra of the fused pyridine analogs **3a–g** exhibit singlets for the CH group of the pyridine ring at ~ 7 ppm and broad peaks due to the NH–functionalities around 12 ppm. In the ^{13}C NMR spectra of the synthesized compounds, the signals observed at δ 160.6–162.0 are assigned to the carbonyl group (C=O). Carbon signals of the methyl group were observed at δ 23.7–23.8 ppm.

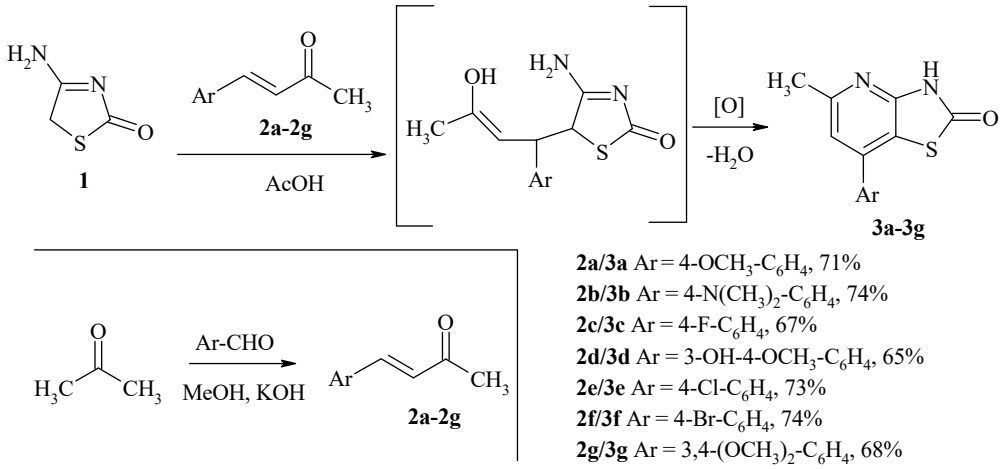

Scheme 1. Synthesis of 5-methyl-7-phenyl-3*H*-thiazolo[4,5-*b*]pyridin-2-ones **3a–g**.

3.2. Biological Activity

Antimicrobial resistance (AMR) is a global healthcare problem, and there is a close interrelationship between the progressing of AMR in the world and the increase in mortality from infectious diseases, mainly through healthcare-associated infections (HAIs) [46]. According to a WHO prognosis, mortality from AMR pathogens in the world by 2050 will take first place in the overall structure of causes of death and will exceed the mortality of cancer. According to the WHO recommendation, discovering new synthetic molecules with antimicrobial action is one of the leading short-term approaches to control AMR pathogens. 4-Thiazolidinone-based derivatives are one of the promising classes of compounds with a polypharmacological profile, which contain several reaction centres in the basic heterocycle and are relatively easily adapted for chemical modification. That is why this class of chemical compounds is useful in the search for a "drug-like molecule" with antimicrobial action, effective against the variable mechanisms of AMR, including HAIs pathogens.

Thus, according to the screening of the antimicrobial activity of 5-methyl-7-phenyl-3*H*-thiazolo[4,5-*b*]pyridin-2-ones, the best activity was shown by the compound **3g**, which showed antifungal activity against fungi of the genus *Candida*, selective action against Gram-positive microorganism *Micrococcus luteus*, and selective action on few Gram-negative microorganisms (Table 1 and Figure 3). In Figure 3, it is shown that compounds **3a** (light blue colour), **3c** (grey colour), **3f** (green colour), and **3g** (dark clue colour) have a bigger growth inhibition zone than solvent control (brown colour).

Compounds **3f** and **3d** exhibited the highest antifungal activity, both for fungi of the genus *Candida* and fungus of the genus *Saccharomyces*. These compounds have also been active against some Gram-negative microorganisms, particularly against clinical strains of *Citrobacter freundii* and *Achromobacter xylosoxidans*.

Four compounds (**3a**, **3c**, **3f**, **3g**) showed significant antimicrobial activity against both clinical and reference Gram-negative microorganisms.

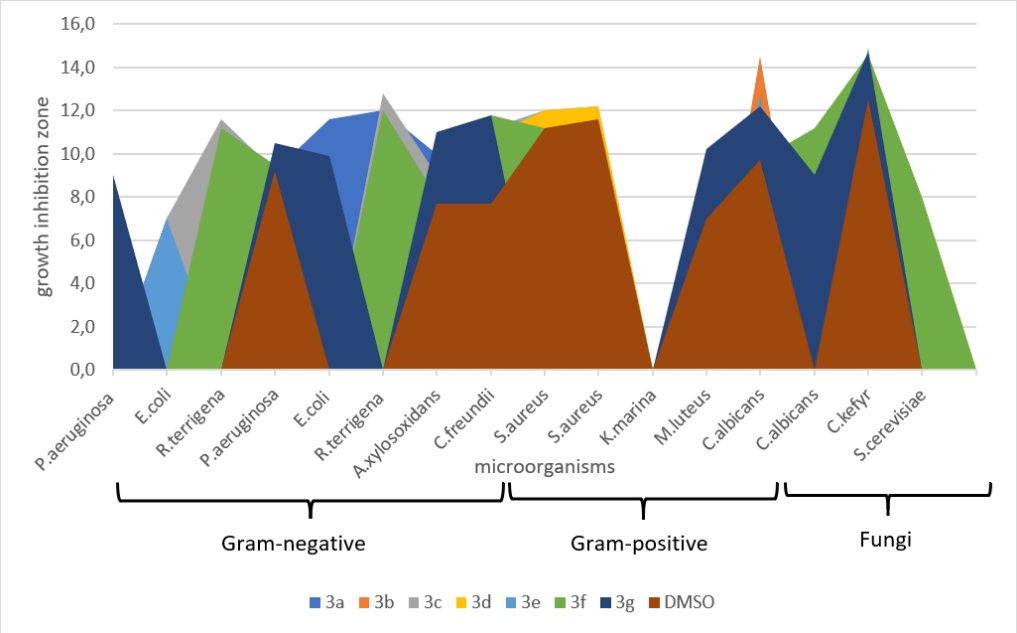

Figure 3. In vitro antimicrobial activity of compounds **3a**–**g**.

The tested compounds did not show significant antimicrobial activity against Gram-positive microorganisms, except for the compound **3g**, active against *Micrococcus luteus*. Four lead-compounds (Table 2) were tested for the minimum inhibitory concentration (MIC). The best activity showed compound **3g** against Gram-negative microorganisms (0.21 μM) and reference strain *Candida albicans* (0.83 μM).

Table 2. MIC value (μM) of compounds against bacterial species.

	μM						
	3a	**3c**	**3f**	**3g**	**Vancomycin**	**Ciprofloxacin**	**Clotrimazole**
Pseudomonas aeruginosa N 7	-	-	1.56	0.21	-	1.81	-
Escherichia coli N 37	1.84	0.96	-	0.21	-	1.51	-
Raoultella terrigena N1	1.84	0.96	0.78	-	-	2.11	-
Citrobacter freundii N 2	-	0.96	1.56	1.66	-	2.26	-
Staphylococcus aureus N 23	-	0.96	-	-	4.16	3.02	-
Micrococcus luteus N 136	-	-	-	1.66	2.77	4.53	-
Candida. albicans (ATCC 885-653)	1.84	0.96	1.56	0.83	-	-	1.16
Candida albicans N 60	1.84	1.92	1.56	1.66	-	-	2.9

'-' not tested.

To know how normal human cells react to synthesized lead-compounds **3c**, **3g**, and **3f**, we tested their toxicity on two human pseudonormal cell lines: human epidermal keratinocytes (HaCat) and normal murine fibroblasts (BALB/c 3T3) (Figure 4). In general, the HaCat cell line is more sensitive than the BALB/c 3T3 cell line to the action of our discovered compounds, but any reaches its IC_{50} value after 72h of compound exposure. The compound **3f** shows the lowest toxicity effect on the pseudonormal cells.

According to obtained results, the tested compound **3g** possesses a low ability to damage pseudonormal cells, had high antifungal activity, and revealed a promising area for further research.

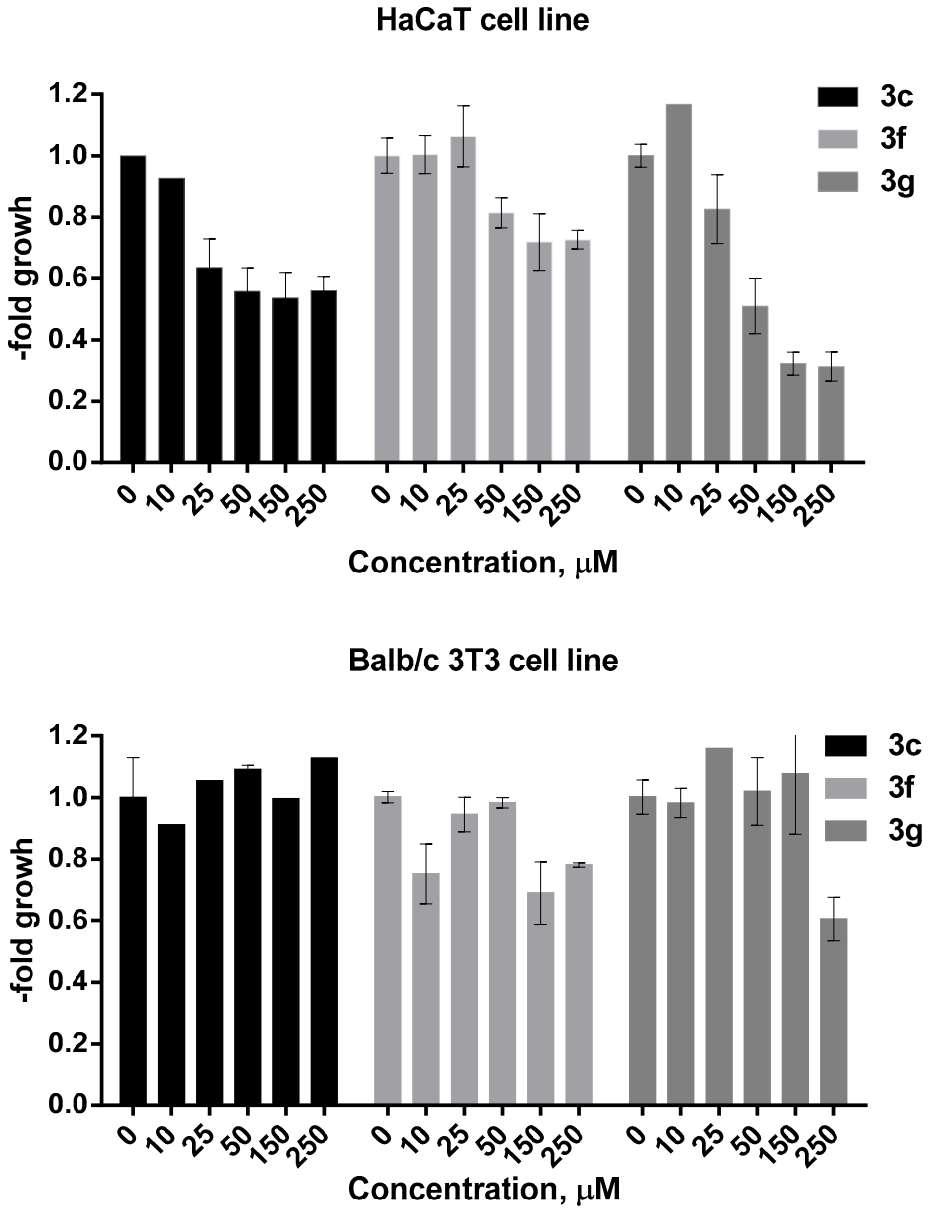

Figure 4. Effect of new thiazolopyridine derivatives with promising antimicrobial and antifungal profile on normal and pseudonormal cells in vitro. Effect of derivatives **3c**, **3f** and **3g** on proliferative activity of HaCat and BALB/c 3T3 cells.

3.3. Molecular and Pharmacokinetic Properties

The physical properties and the ADMET parameters of active compounds **3c**, **3f**, and **3g** were calculated using the SwisAdme online server of the Swiss Institute of Bioinformatics [47]. As suggested by these data, all compounds are suited to Lipinski's rule of five and may exhibit high gastrointestinal absorption and cross the blood–brain barrier (except **3g**). The predicted lipophilicity of synthesized compounds given by log Po/w revealed good permeability and oral absorption through the cell membrane. Our tested compounds did not become *p*-glycoprotein substrates, suggesting that they could not be associated with the excretion of the drug. The negative skin permeability of the tested compounds may exhibit low skin permeation across the cell membrane. All the predictive data allow for the considering of compounds **3f**, **3g**, and **3c** as prospective drug-like candidates in further in-depth studies (Table 3).

Table 3. Physicochemical and pharmacokinetics properties of the active compounds **3f**, **3g**, and **3c**.

	3c	3f	3g
Physicochemical properties			
Molecular weight	260.29	321.19	302.35
Num. heavy atoms	18	18	21
Num. arom. heavy atoms	15	15	15
Num. rotatable bonds	1	1	3
Num. H-bond acceptors	3	2	4
Num. H-bond donors	1	1	1
Molar Refractivity	70.60	78.34	83.63
TPSA Å^2	73.99	73.99	92.45
Consensus log Po/w	3.35	3.67	2.99
Lipinski'Rule	Yes	Yes	Yes
Pharmacokinetics			
GI absorption	High	High	High
BBB permeant	Yes	Yes	No
p-gp substrate	No	No	No
Log Kp (SP) (cm/s) (skin permeation)	−5.71	−5.66	−6.08
Bioavailability Score	0.55	0.55	0.55

3.4. Molecular Docking Studies

Docking studies have revealed that the lead-compound **3g** demonstrated good binding energy towards selected protein targets compared to the reference inhibitor N21 and ciprofloxacin (Table 4).

Table 4. Docking results of **3g** inside MurD (2Y67) and DNA gyrase (2XCT) active sites.

	MurD (2Y67)		DNA Gyrase (2XCT)	
COMPOUND	**Estimated Free Energy of Binding (kcal/mol)**	**Estimated Inhibitory Constant, Ki (μM)**	**Estimated Free Energy of Binding (kcal/mol)**	**Estimated Inhibitory Constant, Ki**
3g	−6.31	23.63 uM	−8.28	858.77 nM
Ciprofloxacin	-	-	−8.35	756.11 nM
N21	−6.08	34.80 uM	-	-

Molecule bonds to the active site of the protein by three hydrogen bonds with the LYS319 (1.92 Å), SER415 (1.87 Å), and ARG425 (3.09 Å). Summary binding energy increases owing to additional Pi–Pi T-shaped, Alkyl, and Pi-Alkyl hydrophobic interaction with the number of lipophilic amino acids ALA414, LEU416, PHE422, ILE 139. Additionally, LYS115, GLU157, and ASN138 form weak carbon–hydrogen bonds with two methoxy groups of **3g**. However, the length of the molecule is quite small, and there is an absence of interaction with THR36, which is quite necessary for efficient MurD inhibition (Figure 5).

The docking results for compound **3g** suggest that these compounds form key interactions with important residues at the binding site DNA gyrase (Figure 6). The compound makes a strong connection inside the active site of DNA gyrase owing to three hydrogen bonds with the SER1084 (1.81 Å), ASP437 (2.01Å), and GLY459 (2.15 Å). Additionally, the position of the molecule is stabilized by Pi–Pi-staked interaction between phenyl, 3*H*-thiazolo[4,5-*b*]pyridine cores and nucleotides DG9 and DT8. Moreover, the 3-methoxy group and the thiazole motif form Pi–Alkyl connections with ARG458 and DG9. Ciprofloxacin also forms a hydrogen bond with SER1084 and Pi–alkyl interaction with ARG458, and interactions with the amino acids, as mentioned above, are crucial for the expression of its antibacterial activity. Binding energies and inhibitory constant are equal to ciprofloxacin results, which suggest the good antibacterial potential of compound **3g**.

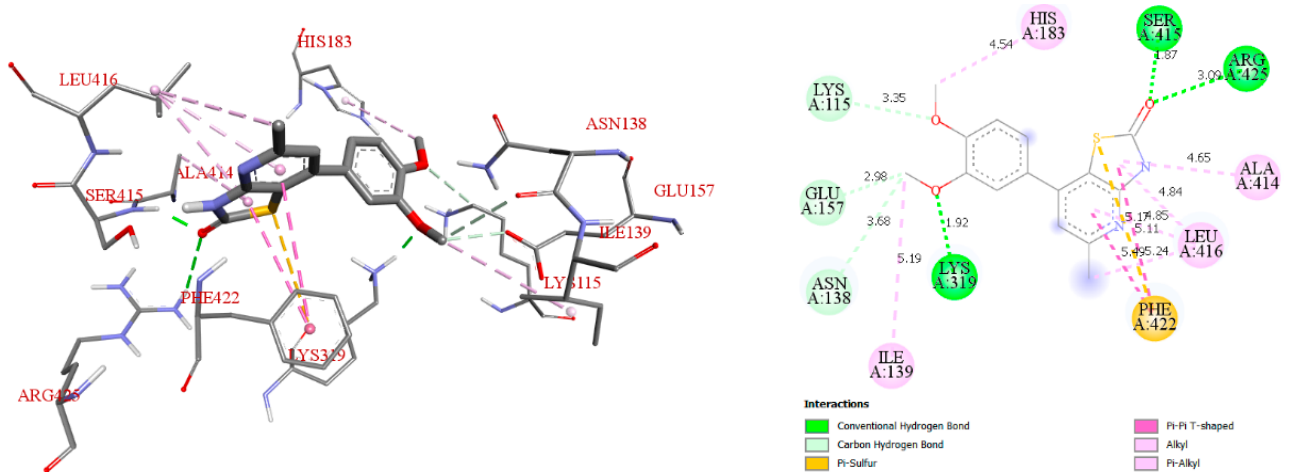

Figure 5. Binding mode of **3g** with MurD (PDB 2Y67).

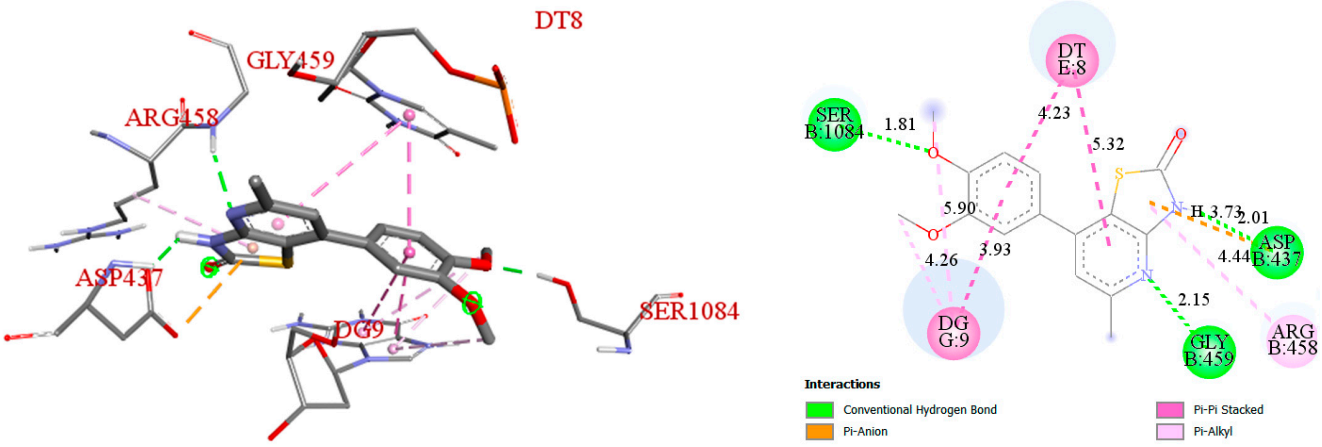

Figure 6. Binding mode of **3g** with DNA gyrase (PDB 2XCT).

4. Conclusions

Novel 5-methyl-7-phenyl-3*H*-thiazolo[4,5-*b*]pyridin-2-ones have been synthesized and characterized by spectral and elementary analyses. The synthesized compounds were assessed for their antimicrobial properties against clinical and reference strains and cytotoxicity capacities against HaCat and BALB/c 3T3 cell lines. The antimicrobial screening led to identifying the active compound **3g** with the highest activity against *Pseudomonas aeruginosa* and *Escherichia coli* (MIC = 0.21 μM). Molecular and pharmacokinetic parameters of the promising active compounds showed satisfactory bioavailability and drug-likeness properties. Computational docking studies of compound **3g** displaying the potent inhibitory effect suggest their good fitting in the active sites of MurD and DNA gyrase via different types of interactions.

Supplementary Materials: The following are available online at https://www.mdpi.com/article/10.3390/scipharm89040052/s1, Figures S1–S18: Copies of ^{1}H, ^{13}C NMR and LC-MS spectra of compounds **3a**–**g**.

Author Contributions: Conceptualization, R.L.; Methodology and experimental work, A.L., Y.K., J.S., O.K., Y.S. and I.Y.; Data Analysis, A.L., Y.K., J.S., D.K. and R.L.; writing—review and editing, A.L., Y.K. and R.L.; Project administration and Supervision, R.L. All authors have read and agreed to the published version of the manuscript.

Funding: The research leading to these results has received funding from the Ministry of Health of Ukraine, under the project number: 0121U100690, and the National Research Foundation of Ukraine, under the project number: 2020.02/0035.

Institutional Review Board Statement: Not applicable.

Informed Consent Statement: Not applicable.

Data Availability Statement: The data presented in this study are available in this article.

Acknowledgments: This research was supported by the Danylo Halytsky Lviv National Medical University, which is gratefully acknowledged. A graphical abstract created with BioRender.com (accessed on 21 September 2021).

Conflicts of Interest: The authors declare no conflict of interest.

References

1. Lukevits, E. Pyridine derivatives in the drug arsenal (150 years of pyridine chemistry). *Chem. Heterocycl. Compd.* **1995**, *31*, 639–650. [CrossRef]
2. Kishbaugh, T.L.S. Pyridines and Imidazopyridines with medicinal significance. *Curr. Top. Med. Chem.* **2016**, *16*, 3274–3302. [CrossRef]
3. Damani, L.A.; Crooks, P.A.; Shaker, M.S.; Caldwell, J.; D'souza, J.; Smith, R.L. Species differences in the metabolic C-and N-oxidation, and N-methylation of [^{14}C] pyridine in vivo. *Xenobiotica* **1982**, *12*, 527–534. [CrossRef] [PubMed]
4. Carlson, G.P. Comparison of the effects of pyridine and its metabolites on rat liver and kidney. *Toxicol. Lett.* **1996**, *85*, 173–178. [CrossRef]
5. Cronin, M.T.D.; Dearden, J.C.; Duffy, J.C.; Edwards, R.; Manga, N.; Worth, A.P.; Worgan, A.D.P. The importance of hydrophobicity and electrophilicity descriptors in mechanistically-based QSARs for toxicological endpoints. *SAR QSAR Environ. Res.* **2002**, *13*, 167–176. [CrossRef] [PubMed]
6. Salem, M.S.; Ali, M.A.M. Novel pyrazolo[3,4-*b*]pyridine derivatives: Synthesis, characterization, antimicrobial and antiproliferative profile. *Biol. Pharm. Bull.* **2016**, *39*, 473–483. [CrossRef]
7. Al-Tel, T.H.; Al-Qawasmeh, R.A.; Zaarour, R. Design, synthesis and in vitro antimicrobial evaluation of novel Imidazo[1,2-*a*]pyridine and imidazo[2,1-*b*][1,3]benzothiazole motifs. *Eur. J. Med. Chem.* **2011**, *46*, 1874–1881. [CrossRef] [PubMed]
8. Arabshahi, H.J.; Van Rensburg, M.; Pilkington, L.I.; Jeon, C.Y.; Song, M.; Gridel, L.M.; Leung, E.; Barker, D.; Vuica-Ross, M.; Volcho, K.P.; et al. A synthesis, in silico, in vitro and in vivo study of thieno[2,3-*b*]pyridine anticancer analogues. *MedChemComm* **2015**, *6*, 1987–1997. [CrossRef]
9. Eissa, I.H.; El-Naggar, A.M.; El-Hashash, M.A. Design, synthesis, molecular modeling and biological evaluation of novel 1*H*-pyrazolo[3,4-*b*]pyridine derivatives as potential anticancer agents. *Bioorg. Chem.* **2016**, *67*, 43–56. [CrossRef]
10. Dias, L.R.; Santos, M.B.; de Albuquerque, S.; Castro, H.C.; de Souza, A.M.; Freitas, A.C.; DiVaio, M.A.; Cabral, L.M.; Rodrigues, C.R. Synthesis, in vitro evaluation, and SAR studies of a potential antichagasic 1*H*-pyrazolo[3,4-*b*]pyridine series. *Bioorg. Med. Chem.* **2007**, *15*, 211–219. [CrossRef]
11. Shi, F.; Li, C.; Xia, M.; Miao, K.; Zhao, Y.; Tu, S.; Zheng, W.; Zhang, G.; Ma, N. Green chemoselective synthesis of thiazolo[3,2-*a*]pyridine derivatives and evaluation of their antioxidant and cytotoxic activities. *Bioorg. Med. Chem. Lett.* **2009**, *19*, 5565–5568. [CrossRef] [PubMed]
12. Al-Omar, M.A.; Youssef, K.M.; El-Sherbeny, M.A.; Awadalla, S.A.A.; El-Subbagh, H.I. Synthesis and in vitro antioxidant activity of some new fused pyridine analogs. *Arch. Pharm.* **2005**, *338*, 175–180. [CrossRef]
13. Abdelgawad, M.A.; Bakr, R.B.; Azouz, A.A. Novel pyrimidine-pyridine hybrids: Synthesis, cyclooxygenase inhibition, anti-inflammatory activity and ulcerogenic liability. *Bioorg. Chem.* **2018**, *77*, 339–348. [CrossRef] [PubMed]
14. Chung, S.T.; Huang, W.H.; Huang, C.K.; Liu, F.C.; Huang, R.Y.; Wu, C.C.; Lee, A.R. Synthesis and anti-inflammatory activities of 4*H*-chromene and chromeno[2,3-*b*]pyridine derivatives. *Res. Chem. Intermed.* **2016**, *42*, 1195–1215. [CrossRef]
15. Witherington, J.; Bordas, V.; Garland, S.L.; Hickey, D.M.; Ife, R.J.; Liddle, J.; Saunders, M.; Smith, D.G.; Ward, R.W. 5-Aryl-pyrazolo[3,4-*b*]pyridines: Potent inhibitors of glycogen synthase kinase-3 (GSK-3). *Bioorg. Med. Chem. Lett.* **2003**, *13*, 1577–1580. [CrossRef]
16. Chioua, M.; Samadi, A.; Soriano, E.; Lozach, O.; Meijer, L.; Marco-Contelles, J. Synthesis and biological evaluation of 3,6-diamino-1*H*-pyrazolo[3,4-*b*]pyridine derivatives as protein kinase inhibitors. *Bioorg. Med. Chem. Lett.* **2009**, *19*, 4566–4569. [CrossRef] [PubMed]
17. Othman, I.M.; Gad-Elkareem, M.A.; Snoussi, M.; Aouadi, K.; Kadri, A. Novel fused pyridine derivatives containing pyrimidine moiety as prospective tyrosyl-tRNA synthetase inhibitors: Design, synthesis, pharmacokinetics and molecular docking studies. *J. Mol. Struct.* **2020**, *1219*, 128651. [CrossRef]
18. Sun, Q.Z.; Lin, G.F.; Li, L.L.; Jin, X.T.; Huang, L.Y.; Zhang, G.; Yang, W.; Chen, K.; Xiang, R.; Chen, C.; et al. Discovery of potent and selective inhibitors of cdc2-like kinase 1 (clk1) as a new class of autophagy inducers. *J. Med. Chem.* **2017**, *60*, 6337–6352. [CrossRef]
19. Fujita, M.; Seki, T.; Ikeda, N. Synthesis and bioactivities of novel bicyclic thiophenes and 4,5,6,7-tetrahydrothieno[2,3-*c*]pyridines as inhibitors of tumor necrosis factor-α (TNF-α) production. *Bioorg. Med. Chem. Lett.* **2002**, *12*, 1897–1900. [CrossRef]
20. Das, D.; Sikdar, P.; Bairagi, M. Recent developments of 2-aminothiazoles in medicinal chemistry. *Eur. J. Med. Chem.* **2016**, *109*, 89–98. [CrossRef]

21. Bondock, S.; Albormani, O.; Fouda, A.M.; Abu Safieh, K.A. Progress in the chemistry of 5-acetylthiazoles. *Synth. Commun.* **2016**, *46*, 1081–1117. [CrossRef]
22. Chebanov, V.A.; Saraev, V.E.; Desenko, S.M.; Chernenko, V.N.; Knyazeva, I.V.; Groth, U.; Glasnov, T.N.; Kappe, C.O. Tuning of chemo-and regioselectivities in multicomponent condensations of 5-aminopyrazoles, dimedone, and aldehydes. *J. Org. Chem.* **2008**, *73*, 5110–5118. [CrossRef] [PubMed]
23. Chebanov, V.A.; Sakhno, Y.I.; Desenko, S.M.; Chernenko, V.N.; Musatov, V.I.; Shishkina, S.V.; Shishkin, O.V.; Kappe, C.O. Cyclo-condensation reactions of 5-aminopyrazoles, pyruvic acids and aldehydes. Multicomponent approaches to pyrazolopyridines and related products. *Tetrahedron* **2007**, *63*, 1229–1242. [CrossRef]
24. Chebanov, V.A.; Desenko, S.M. Dihydroazines based on α,β-unsaturated ketones reactions. *Curr. Org. Chem.* **2006**, *10*, 297. [CrossRef]
25. Lozynskyi, A.; Zimenkovsky, B.; Radko, L.; Stypula-Trebas, S.; Roman, O.; Gzella, A.K.; Lesyk, R. Synthesis and cytotoxicity of new thiazolo[4,5-*b*]pyridine-2(3*H*)-one derivatives based on α,β-unsaturated ketones and α-ketoacids. *Chem. Pap.* **2018**, *72*, 669–681. [CrossRef]
26. Lozynskyi, A.; Zimenkovsky, B.; Gzella, A.K.; Lesyk, R. Arylidene pyruvic acids motif in the synthesis of new 2*H*,5*H*-chromeno [4′,3′:4,5]thiopyrano[2,3-*d*]thiazoles via tandem hetero-Diels–Alder-hemiacetal reaction. *Synth. Commun.* **2015**, *45*, 2266–2270. [CrossRef]
27. Lozynskyi, A.; Zimenkovsky, B.; Nektegayev, I.; Lesyk, R. Arylidene pyruvic acids motif in the synthesis of new thiopyrano[2,3-*d*] thiazoles as potential biologically active compounds. *Heterocycl. Commun.* **2015**, *21*, 55–59. [CrossRef]
28. Lozynskyi, A.; Zasidko, V.; Atamanyuk, D.; Kaminskyy, D.; Derkach, H.; Karpenko, O.; Ogurtsov, V.; Kutsyk, R.; Lesyk, R. Synthesis, antioxidant and antimicrobial activities of novel thiopyrano[2,3-*d*]thiazoles based on aroylacrylic acids. *Mol. Divers.* **2017**, *21*, 427–436. [CrossRef]
29. Khodarahmi, G.; Asadi, P.; Farrokhpour, H.; Hassanzadeh, F.; Dinari, M. Design of novel potential aromatase inhibitors via hybrid pharmacophore approach: Docking improvement using the QM/MM method. *RSC Adv.* **2015**, *5*, 58055–58064. [CrossRef]
30. Chaban, T.I.; Ogurtsov, V.V.; Chaban, I.G.; Klenina, O.V.; Komarytsia, J.D. Synthesis and antioxidant activity evaluation of novel 5,7-dimethyl-3*H*-thiazolo[4,5-*b*]pyridines. *Phosphorus Sulfur Silicon Relat. Elem.* **2013**, *188*, 1611–1620. [CrossRef]
31. Chaban, T.I.; Ogurtsov, V.V.; Matiychuk, V.S.; Chaban, I.G.; Demchuk, I.L.; Nektegayev, I.A. Synthesis, anti-inflammatory and antioxidant activities of novel 3*H*-thiazolo[4,5-*b*]pyridines. *Acta Chim. Slov.* **2019**, *66*, 103–111. [CrossRef] [PubMed]
32. El-Gaby, M.S.A.; Al-Sehemi, A.G.; Mohamed, Y.A.; Ammar, Y.A. Recent trends in chemistry of thiazolopyridines. *Phosphorus Sulfur Silicon Relat. Elem.* **2006**, *181*, 631–674. [CrossRef]
33. Hegde, S.G.; Mahoney, M.D. Synthesis and herbicidal activity of 5-(haloalkyl)-substituted thiazolo[4,5-*b*]pyridine-3(2*H*)-acetic acid derivatives. *J. Agric. Food Chem.* **1993**, *41*, 2131–2134. [CrossRef]
34. Lozynskyi, A.; Zimenkovsky, B.; Ivasechko, I.; Senkiv, J.; Gzella, A.; Karpenko, O.; Stoika, R.; Lesyk, R. Synthesis and cytotoxicity of new 2-oxo-7-phenyl-2,3-dihydrothiazolo[4,5-*b*]pyridine-5-carboxylic acid amides. *Phosphorus Sulfur Silicon Relat. Elem.* **2019**, *194*, 1149–1157. [CrossRef]
35. Lozynskyi, A.V.; Derkach, H.O.; Zasidko, V.V.; Konechnyi, Y.T.; Finiuk, N.S.; Len, Y.T.; Kutsyk, R.V.; Regeda, M.S.; Lesyk, R.B. Antimicrobial and cytotoxic activities of thiazolo[4,5-*b*]pyridine derivatives. *Biopolym. Cell* **2021**, *37*, 153. [CrossRef]
36. Komaritsa, I.D. Studies on azolidones and their derivatives. *Chem. Heterocycl. Compd.* **1968**, *4*, 324–325. [CrossRef]
37. Skrobiszewski, A.; Ogórek, R.; Pląskowska, E.; Gładkowski, W. *Pleurotus ostreatus* as a source of enoate reductase. *Biocatal. Agric. Biotechnol.* **2013**, *2*, 26–31. [CrossRef]
38. EUCAST. Disk Diffusion—Manual v 8.0 (1 January 2020). Available online: http://www.eucast.org/fileadmin/src/media/PDFs/EUCAST_files/Disk_test_documents/2020_manuals/Manual_v_8.0_EUCAST_Disk_Test_2020.pdf (accessed on 20 July 2021).
39. Balouiri, M.; Sadiki, M.; Ibnsouda, S.K. Methods for in vitro evaluating antimicrobial activity: A review. *J. Pharm. Anal.* **2016**, *6*, 71–79. [CrossRef]
40. Tomašić, T.; Zidar, N.; Rupnik, V.; Kovač, A.; Blanot, D.; Gobec, S.; Kikelj, D.; Mašič, L.P. Synthesis and biological evaluation of new glutamic acid-based inhibitors of MurD ligase. *Bioorg. Med. Chem. Lett.* **2009**, *19*, 153–157. [CrossRef]
41. Tomasic, T.; Katsamakas, S.; Hodnik, Z.; Ilaš, J.; Brvar, M.; Solmajer, T.; Montalvão, S.; Tammela, P.; Banjanac, M.; Ergović, G.; et al. Discovery of 4, 5, 6, 7-tetrahydrobenzo[1,2-*d*]thiazoles as novel DNA gyrase inhibitors targeting the ATP-binding site. *J. Med. Chem.* **2015**, *58*, 5501–5521. [CrossRef]
42. Zidar, N.; Tomašić, T.; Šink, R.; Kovač, A.; Patin, D.; Blanot, D.; Contreras-Martel, C.; Dessen, A.; Premru, M.M.; Zega, A.; et al. New 5-benzylidenethiazolidin-4-one inhibitors of bacterial MurD ligase: Design, synthesis, crystal structures, and biological evaluation. *Eur. J. Med. Chem.* **2011**, *46*, 5512–5523. [CrossRef] [PubMed]
43. Bax, B.D.; Chan, P.F.; Eggleston, D.S.; Fosberry, A.; Gentry, D.R.; Gorrec, F.; Giordano, I.; Hann, M.M.; Hennessy, A.; Hibbs, M.; et al. Type IIA topoisomerase inhibition by a new class of antibacterial agents. *Nature* **2010**, *466*, 935–940. [CrossRef] [PubMed]
44. Morris, G.M.; Huey, R.; Lindstrom, W.; Sanner, M.F.; Belew, R.K.; Goodsell, D.S.; Olson, A.J. AutoDock4 and AutoDockTools4: Automated docking with selective receptor flexibility. *J. Comput. Chem.* **2009**, *30*, 2785–2791. [CrossRef] [PubMed]
45. Morris, G.M.; Goodsell, D.S.; Halliday, R.S.; Huey, R.; Hart, W.E.; Belew, R.K.; Olson, A.J. Automated docking using a Lamarckian genetic algorithm and an empirical binding free energy function. *J. Comput. Chem.* **1998**, *19*, 1639–1662. [CrossRef]
46. Aiken, A.M.; Allegranzi, B.; Scott, J.A.; Mehtar, S.; Pittet, D.; Grundmann, H. Antibiotic resistance needs global solutions. *Lancet Infect. Dis.* **2014**, *14*, 550–551. [CrossRef]
47. SwissADME. Available online: http://www.swissadme.ch/ (accessed on 27 March 2021).